Review of Scientific Instruments

Multi-mode resistive spectroscopy for precisely controlling morphology of extremely narrow gap palladium nanocluster array

Cite as: Rev. Sci. Instrum. **92**, 063901 (2021); https://doi.org/10.1063/5.0049536
Submitted: 05 March 2021 • Accepted: 10 May 2021 • Published Online: 01 June 2021

N. Nakamura, K. Kashiuchi and H. Ogi

Review of Scientific Instruments ARTICLE scitation.org/journal/rsi

Multi-mode resistive spectroscopy for precisely controlling morphology of extremely narrow gap palladium nanocluster array

Cite as: Rev. Sci. Instrum. 92, 063901 (2021); doi: 10.1063/5.0049536
Submitted: 5 March 2021 • Accepted: 10 May 2021 •
Published Online: 1 June 2021

N. Nakamura,[1,a)] K. Kashiuchi,[1] and H. Ogi[2]

AFFILIATIONS

[1] Graduate School of Engineering Science, Osaka University, 1-3 Machikaneyama, Toyonaka, Osaka 560-8531, Japan
[2] Graduate School of Engineering, Osaka University, 2-1 Yamadaoka, Suita, Osaka 565-0871, Japan

[a)] **Author to whom correspondence should be addressed:** nobutomo@me.es.osaka-u.ac.jp

ABSTRACT

During the deposition of a metallic material on a substrate, a nanocluster-array structure with an extremely narrow gap is formed transiently at the transition between isolated clusters and the continuous film. It is known that the nanocluster array shows a unique electrical property different from that of isolated clusters and the continuous film. The electrical property of the nanocluster array changes significantly depending on its morphology, and precise control of the deposition time is indispensable to obtain a desired electrical property. However, the detection of the transition is not straightforward. To overcome this problem, we develop the multi-mode resistive spectroscopy. It evaluates the morphological change during deposition using resonant vibrations of a piezoelectric material and enables the fabrication of nanocluster arrays with a slightly different morphology. Palladium nanocluster arrays with different morphologies are fabricated using this method, and the availability of the multi-mode resistive spectroscopy is demonstrated by evaluating their electrical response to hydrogen gas.

I. INTRODUCTION

When a metallic material is deposited on a substrate, isolated nanoclusters are formed in the early stage of deposition, and after they grow and contact with each other, the continuous film is formed. During the film growth process, the electrical resistance of the deposited metal decreases drastically depending on the morphology.[1–3] Therefore, by interrupting deposition at a certain time, a nanostructure (nanoclusters or the continuous film) with a desired resistance is obtained.

Among nanostructures, we here focus on the nanocluster array that appears in the transition between isolated nanoclusters and the subsequent continuous film. In the nanocluster array, because some clusters are isolated with an extremely narrow gap and others are contacting with each other, it shows an intermediate resistance between an insulator and a conductor. The electrical property of the nanocluster array is quite sensitive to the gap distance and fraction of isolated and contacting clusters. For example, in the palladium-nanocluster-based hydrogen-gas sensor,[4–7] which is a representative application of the nanocluster array, a slight difference in the deposition time causes a remarkable change in the sensing mechanism as shown in this study. Therefore, to fabricate a nanocluster array, it is important to monitor the morphological change during deposition and interrupt the deposition at an appropriate moment.

The morphological change during deposition has been monitored using the resistance measurement,[1,8] the curvature measurement,[9–11] a combination of surface differential reflectance spectroscopy and the multiple-beam optical stress sensor,[12] a combination of the curvature measurement, spectroscopic ellipsometry, and the resistance measurement,[13] and resistive spectroscopy.[14,15] The resistive spectroscopy is more sensitive to the morphological change around the transition, and it is, therefore, suitable for fabricating the nanocluster arrays. It evaluates the morphological change using a resonant vibration of a piezoelectric material placed beneath the substrate. Without contacting the nanocluster nor the substrate, the moment of the transition is precisely identified by monitoring the vibrational loss, which shows a peak at the transition. By detecting the transition using this method, a nanocluster array is obtained by interrupting the deposition at a proper moment. However, there was a difficulty in the control of the gap distance. Using the resistive spectroscopy, making the gap narrower is somewhat easy because it is performed by interrupting the deposition just after

the loss peak is detected. However, to make the gap slightly wider, deposition must be interrupted before the loss peak is detected, but it is difficult to know when the loss peak appears. To overcome this problem, we here develop the multi-mode resistive spectroscopy. In this method, two or more resonant vibrations of the piezoelectric resonator are simultaneously monitored, and the morphological change that occurs within less than 1-nm thickness change is detected.

In this study, the advantage of the developed method over the conventional method is confirmed by fabricating palladium nanocluster arrays and evaluating their electrical response to hydrogen gas. When palladium is exposed to hydrogen gas, the electrical resistance and the volume increase due to the hydrogen absorption. Using these characteristics, palladium-based hydrogen-gas sensors, including the nanocluster-array-based sensor, have been developed.[4–7,16–21] In the nanocluster-array-based sensor, hydrogen gas is detected from the change in the electrical resistance of the nanocluster array. The resistance change is caused mainly by two mechanisms: (i) decrease in the tunneling current between isolated nanoclusters by the hydrogen adsorption and (ii) gap closing between nanoclusters caused by the volume increment by the hydrogen absorption. When the gap between clusters is somewhat wide, the former mechanism becomes dominant and the resistance increases in hydrogen gas. When the gap becomes extremely narrow, the latter mechanism becomes dominant and the resistance decreases. Thus, the response of a palladium nanocluster array to hydrogen gas is sensitive to the gap distance, and precise control of the deposition time is indispensable to obtain an optimum response.

II. EXPERIMENTAL SETUP

Figure 1 shows a schematic image of the mechanism of the resistive spectroscopy. The metallic material is deposited onto the substrate, and the piezoelectric plate vibrating at a resonant frequency is placed below the substrate. The vibrating piezoelectric plate excites the electric field around it, causing the current flow in the deposited material. The current flow spends a part of the vibrational energy of the piezoelectric plate, increasing the vibrational loss. During deposition, the loss shows a maximum when the morphological transition occurs.[14] Therefore, by monitoring the change in the loss, we can identify the moment of the transition. The change in the loss is monitored by obtaining resonant spectra repeatedly around a resonant frequency and measuring the full-width at half maximum (FWHM). Vibrations of the piezoelectric plate are excited

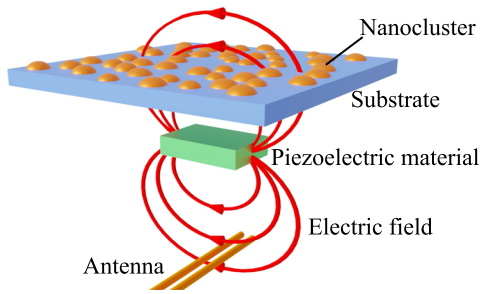

FIG. 1. Schematic image of the mechanism of the resistive spectroscopy.

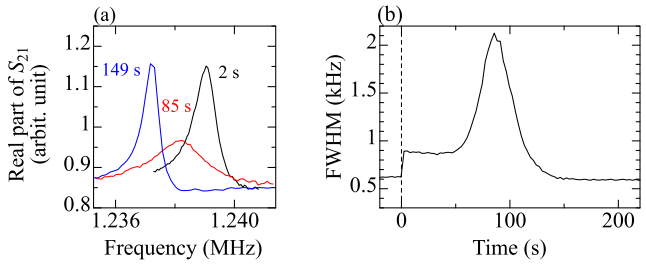

FIG. 2. (a) Resonant spectra measured at different times after starting the deposition. (b) Corresponding FWHM change during the deposition. The dashed line indicates start time of the deposition.

and detected by using line antennas[22] and a network analyzer. The piezoelectric plate used here is a rectangular parallelepiped lithium niobate, measuring 2.5 × 1.7 × 0.2 mm^3 along the crystallographic X, Y, and Z axes, respectively. Details of the experimental setup are described in Ref. 14.

Figure 2 shows representative resonant spectra measured at different times during the deposition of palladium on MgO. In the figure, a resonant mode around 1.238 MHz is monitored. Just after starting the deposition, the resonant peak appears clearly. As the deposition progresses, the peak becomes broader and the FWHM increases. After the FWHM shows a maximum value at 85 s, the resonant peak becomes sharp again. When a resonant spectrum is measured using the antennas, some resonant peaks appear in the spectrum, and the amplitude differs for each resonant mode. Among the peaks, we selected three peaks, including the peak around 1.2 MHz, that appear clearly at different frequency bands, and their FWHM was monitored in the following experiments.

Palladium was deposited on the MgO(001) single crystal substrate with a thickness of 0.3 mm by the RF magnetron sputtering. Background pressure was lower than 4.0 × 10^{-4} Pa, and Ar pressure during deposition was 0.8 Pa.

After fabricating the palladium nanocluster array, to measure their electrical response to hydrogen gas, aluminum wires were attached to the surface by the wire bonding. The sample was placed in a home made hydrogen flow cell, and electric resistance was measured with the two-terminal method. Nitrogen gas was flowed into the cell at 117 ml/min as the carrier gas. The hydrogen detection was performed by mixing hydrogen gas with the carrier gas using a syringe pump. The hydrogen gas is composed of 0.1% hydrogen and 99.9% nitrogen, and its flow rate is 13 ml/min. Therefore, during the hydrogen flow, the hydrogen concentration was 100 ppm and the flow rate was 130 ml/min in the cell. The duration time of the hydrogen flow was 231 s. All experiments were performed at room temperature. Before the hydrogen-gas injection, nitrogen gas was injected to the carrier gas as the control experiment.

III. SINGLE-MODE RESISTIVE SPECTROSCOPY

First, we fabricated two palladium nanocluster arrays (array I and array II) using the conventional resistive spectroscopy in which the FWHM of a resonant mode around 26 MHz was monitored during deposition. Figures 3(a) and 3(b) show the FWHM change during the deposition. Two nanocluster arrays were fabricated by

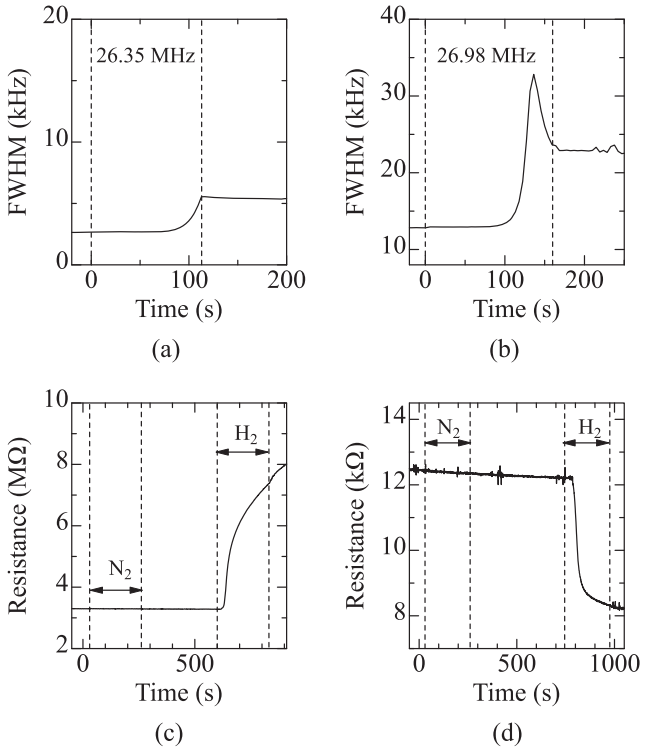

FIG. 3. Change in the FWHM during deposition of two palladium nanocluster arrays [(a) array I and (b) array II], and their electric response to nitrogen and hydrogen gases [(c) array I and (d) array II], respectively.

interrupting the deposition during the increase in the FWHM (array I) and after it showed the peak (array II). After interrupting the deposition, the FWHM sometimes changes with time due to the morphological change in the deposited material.[15] However, notable change in the FWHM was not observed in the present study. The response of the two arrays to the hydrogen gas is shown in Figs. 3(c) and 3(d). In both nanocluster arrays, notable resistance change was not observed during the nitrogen-gas flow. In contrast, the resistance increased in array I, while it decreased in array II during the hydrogen-gas flow. These results indicate that the mechanism of the hydrogen-gas detection changes around the FWHM peak: The tunneling-current change increases the resistance before the FWHM peak, and the gap closing decreases the resistance after the FWHM peak.

IV. MULTI-MODE RESISTIVE SPECTROSCOPY

A. Model calculation using the equilibrium circuit

The gap in the nanocluster array near the FWHM peak thus drastically affects the sensor performance, and it is very important to know the time for peak appearance. However, we could not expect when the FWHM peak appears, and it is difficult to interrupt the deposition just before the FWHM peak. In this study, we find that this difficulty is solved by simultaneously monitoring two or more resonant modes. We call this method the multi-mode resistive spectroscopy. The principle of this method is discussed below using the equilibrium circuit.

In the resistive spectroscopy, a resonant spectrum is obtained by measuring the strength of the electric field excited by the vibrating piezoelectric material with changing the vibration frequency. This experiment can be reproduced by the equilibrium circuit in Fig. 4(a).[14] This circuit reproduces the setup in Fig. 1, and the

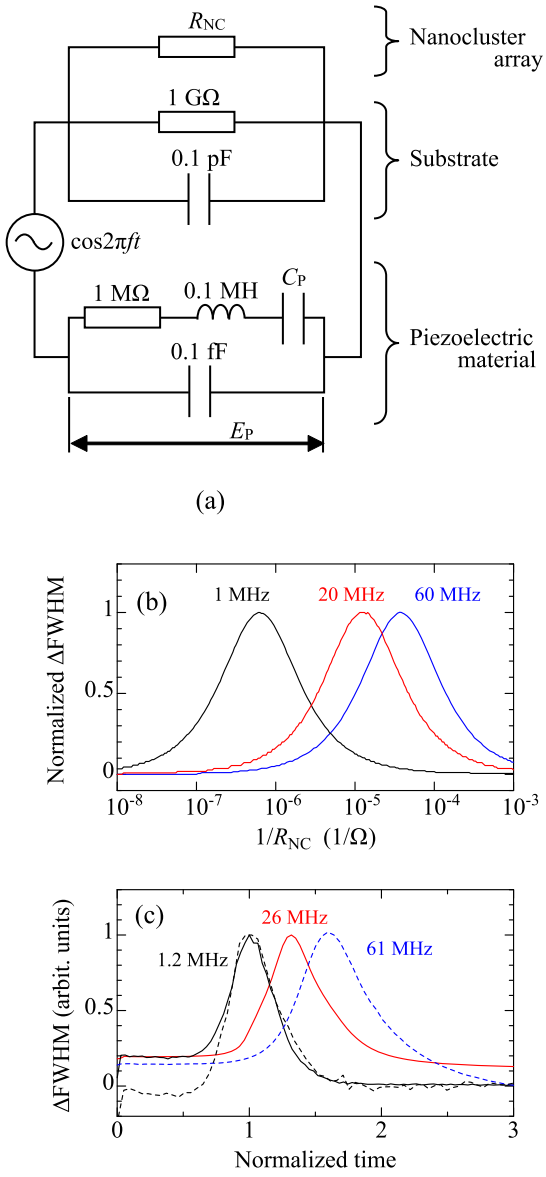

FIG. 4. (a) The equilibrium circuit of the measurement setup. (b) Relationship between the resistance of nanoclusters and the FWHM for different resonant modes calculated using the equilibrium circuit. (c) Change in the FWHM observed during the deposition of two samples. Resonant modes around 1.2 and 26 MHz were measured for a sample (solid curves), and resonant modes around 1.2 and 61 MHz were measured for another sample (dashed curves). The horizontal axis is normalized by the time at which the FWHM of the 1.2-MHz mode shows a peak.

resonant spectrum is obtained by calculating the potential difference E_P in a piezoelectric material with changing the frequency f. The change in the FWHM during deposition is then simulated by measuring the FWHM of the calculated resonant spectrum with decreasing electrical resistance R_{NP} of the nanocluster array.

Figure 4(b) shows the change in the FWHM obtained by the model calculation. The change in the FWHM is normalized so that the maximum and minimum values become 1 and 0, respectively. In the calculation, parameters in Fig. 4(a) were used. C_P was changed to be 2.533×10^{-19}, 6.333×10^{-22}, and 7.036×10^{-23} F so that the resonant frequency f_0 of the piezoelectric material becomes 1, 20, and 60 MHz, respectively. In the calculation results, as the resistance of the nanocluster array decreases, the FWHM increases and shows a peak. As the resonant frequency increases, the FWHM peak appears at a smaller resistance.

In the experiment using the single-mode resistive spectroscopy, it was found that the hydrogen-sensing mechanism changes around the FWHM peak of the 26-MHz mode. This result indicates that the FWHM peak of the 26-MHz mode will be an indicator to select the operating mechanism of the hydrogen sensor; the tunneling-current based sensor and gap-closing based sensor are obtained by interrupting the deposition before and after the FWHM peak, respectively. However, it was difficult to estimate when the FWHM peak appears during deposition. Therefore, monitoring of a single resonant mode was not enough to obtain a desired hydrogen sensor. According to the model calculation, the FWHM peak of the 1-MHz mode appears earlier than the peak of the 26-MHz mode. Therefore, the appearance of the FWHM peak of the lower (1 MHz) mode can be a pre-signal for the FWHM peak of the higher (26 MHz) mode. Usage of two or more resonant modes thus should be helpful for the precise control of the morphology of the nanocluster arrays.

To confirm the validity of this mechanism and availability of the multi-mode resistive spectroscopy, we performed two experiments. In the first experiment, two resonant modes around 1.2 and 26 MHz were monitored during deposition, and in the second experiment, two resonant modes around 1.2 and 61 MHz were monitored. The results are shown in Fig. 4(c). The horizontal axis is normalized so that the FWHM peak of the 1.2-MHz mode appears at 1 since the time at which the FWHM peak appears differs in each deposition: 85.5 s in the first experiment and 100 s in the second experiment. A FWHM peak of the 26-MHz mode appears later than that of the 1.2-MHz mode, and a peak of the 61-MHz mode appears later than them. This behavior shows good agreement with the model calculation, confirming the validity of the model calculation and concept of the multi-mode resistive spectroscopy.

B. Fabrication of palladium nanocluster arrays

Eight palladium nanocluster arrays, named sample 1 to sample 8, were prepared referring to the changes in FWHM values of resonant modes around 1.2 and 26 MHz. For measuring the FWHM, resonant spectra around 1.2 and 26 MHz were measured alternately. Deposition times for fabricating the samples are listed in Table I. One sample was fabricated in each deposition. The deposition rate was 0.027 nm/s, and the thickness of the nanocluster arrays ranged from 2.9 to 5.0 nm.

TABLE I. Deposition time, time at the FWHM peak of the 1.2-MHz mode, and the change ratio of the resistance measured in the hydrogen-detection experiment.

Sample number	Deposition time (s)	Time at FWHM peak (s)	$\Delta R/R$ (%)
1	109	90	119.5
2	124	100	64.9
3	112	84	19.5
4	147	99	39.6
5	150	93	−38.3
6	125	89	−29.9
7	159	115	−27.0
8	184	109	−29.8

Figure 5 shows the FWHM change for the representative two samples. In both samples, the FWHM peak of the 1.2-MHz mode appears earlier than that of the 26-MHz mode as expected. In Fig. 6, the timing at which depositions were interrupted to fabricate the eight nanocluster arrays is plotted on the data shown in Fig. 4(c). Note that the peak appearance time is not exactly the same for each experiment. Experimental conditions were controlled to be the same, but the peak time varied between 84 and 115 s as shown in Table I; fluctuation in the peak time was inevitable due to slight difference in the conditions. Therefore, the data are plotted referring to the relative position to the FWHM peak in Fig. 6. For example, sample 7 was fabricated by interrupting deposition just after the FWHM peak of the 26-MHz mode appears, and the time was at 159 s [Fig. 5(b)]. In Fig. 6(b), the sample is plotted just after the FWHM peak, but the time is not at 159 s.

C. Hydrogen-gas detection

Figure 7 summarizes the change ratio of the resistance after the hydrogen flow for 231 s. In Fig. 7(a), the change ratio is plotted against the deposition time. The change ratio changes from positive values to the negative values as the deposition time increases, and the

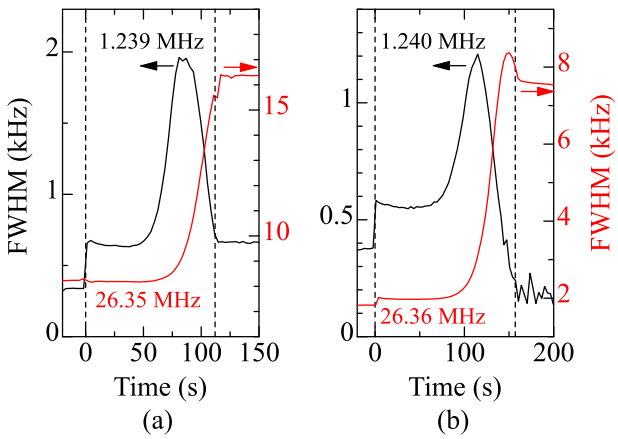

FIG. 5. Change in the FWHM during the deposition of (a) sample 3 and (b) sample 7. Palladium was deposited during the time between the two dashed lines.

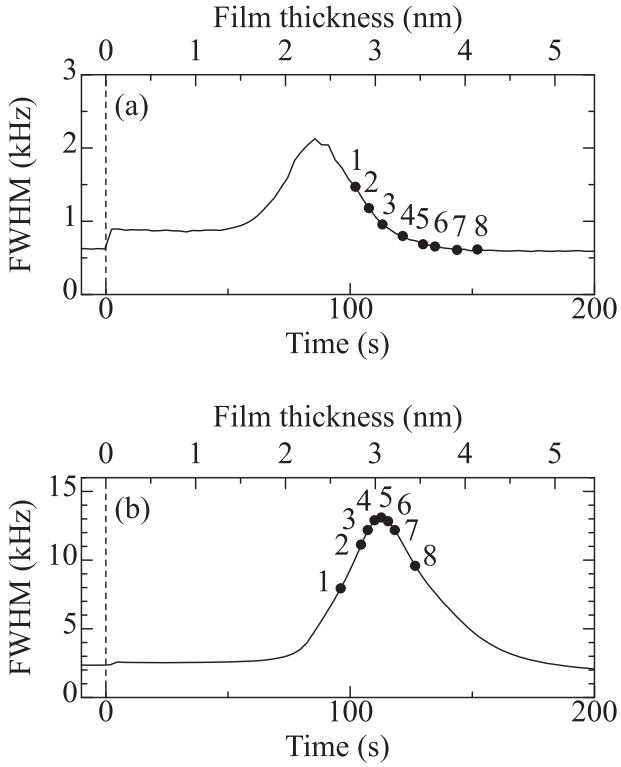

FIG. 6. The time at which the deposition was interrupted is plotted on the FWHM of the (a) 1.2-MHz mode and (b) 26-MHz mode in Fig. 4(c) (solid curves).

transition of the mechanism from the tunneling current to the gap closing is observed around 130 s. However, it is difficult to identify clearly the transition time in Fig. 7(a).

In Fig. 7(b), the change ratio is plotted against the sample number. The change ratio decreases as the sample number increases, and it changes from positive values to negative values between samples 4 and 5. The transition of the resistance-change mechanism clearly appears in this figure. These results indicate that monitoring of the FWHM is more efficient than that of the deposition time. As seen in Table I, the time at which the FWHM peak appears varied between 84 and 115 s in each deposition. Therefore, deposition time cannot be necessarily used for evaluating the morphology of the deposited nanocluster arrays. In contrast, the FWHM reflects the morphological change, and the FWHM peak of the 26-MHz mode indicates the transition of the mechanism.

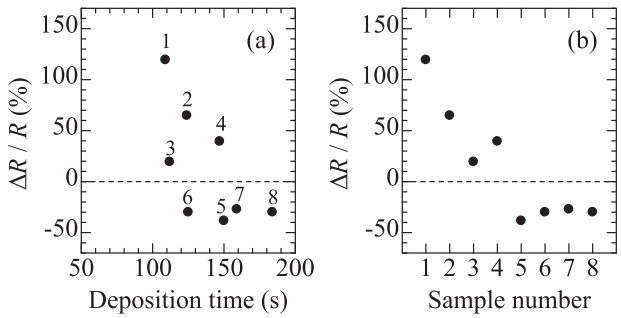

FIG. 7. Change ratio of the electric resistance after exposure to 100-ppm hydrogen gas for 231 s. The horizontal axis of (a) is the deposition time and that of (b) is the sample number. The sample number is indicated in (a).

From these results, if one wants to fabricate a gap-closing based hydrogen sensor (samples 5–8), the sensor is obtained by interrupting the deposition after the FWHM peak of the 26-MHz resonant mode appears. When one wants to fabricate a tunneling-current based hydrogen sensor (samples 1–4), it is obtained by interrupting deposition after the FWHM peak of the 1.2-MHz mode appears.

By monitoring two resonant modes, we could control the morphology and hydrogen-detection mechanism. However, by selecting resonant modes more carefully, the morphology of the nanocluster array will be controlled more precisely. Regarding the gap-closing based hydrogen sensor, the change ratio of the resistance becomes maximum when the deposition is interrupted at the FWHM peak of the 26-MHz resonant mode (sample 5). Because it is difficult to identify the moment at which the FWHM peak appears during deposition, the 1.2-MHz mode was monitored together with the 26-MHz mode. However, the time interval between the FWHM peaks of the 1.2 and 26-MHz modes was somewhat large, and the 1.2-MHz mode was not necessarily suitable for fabricating sample 5. If a resonant mode with a slightly lower resonant frequency than the 26-MHz mode, for example, around 20 MHz, is monitored instead of the 1.2-MHz mode, its FWHM peak will appear just before the FWHM peak of the 26-MHz mode appears. Then, an optimized gap-closing based hydrogen sensor is obtained by interrupting the deposition just after the FWHM peak of the lower mode (~ 20 MHz) appears. Regarding the tunneling-current based hydrogen sensor, the change ratio of the resistance increased as the deposition time became shorter, and timing of interruption is important. These sensors were obtained by interrupting deposition after the FWHM peak of the 1.2-MHz mode appeared and the FWHM of the 26-MHz mode started to increase. In this case, it is also necessary to wait for a while after the FWHM peak of the 1.2-MHz mode appeared before interrupting the deposition. Therefore, a resonant mode whose frequency is higher than 1.2 MHz should be used for controlling the morphology and response to hydrogen of the tunneling-current based sensors. Thus, by selecting proper resonant modes and monitoring their FWHM, a palladium nanocluster array possessing precisely controlled morphology and hydrogen-gas response is obtained.

V. CONCLUSIONS

We developed the multi-mode resistive spectroscopy and demonstrated that it enables the control of the response of a palladium nanocluster array to hydrogen gas. Two resonant modes were monitored in this study, but by monitoring three or more resonant modes, the morphology and electrical properties of nanocluster arrays will be adjusted more precisely. In this study, we confirmed that the FWHM peak appears at different times depending on the resonant mode. The FWHM peak generally appears around the morphological transition from the discontinuous clusters to the continuous film. Therefore, there will be a resonant mode whose FWHM peak indicates the percolation. Finding the resonant mode

will contribute to the research on the evolution of the morphology during deposition.

In the fabrication of the nanocluster array using the multi-mode resistive spectroscopy, the electric field generated by the oscillating piezoelectric material may affect the morphology of the nanocluster array. The effect of the electric field on the morphology will be investigated for controlling the morphology of the nanocluster array more precisely in future work. We hope that the multi-mode resistive spectroscopy and the morphology-controlled nanocluster array are applied to more than just hydrogen sensors in the future.

ACKNOWLEDGMENTS

This research was supported partially by the JSPS KAKENHI (Grant Nos. 18H01883 and 20K21145).

DATA AVAILABILITY

The data that support the findings of this study are available from the corresponding author upon reasonable request.

REFERENCES

[1] I. M. Rycroft and B. L. Evans, Thin Solid Films **290-291**, 283 (1996).
[2] S. K. So, H. H. Fong, C. F. Yeung, and N. H. Cheung, Appl. Phys. Lett. **77**, 1099 (2000).
[3] K. Seal, M. A. Nelson, Z. C. Ying, D. A. Genov, A. K. Sarychev, and V. M. Shalaev, Phys. Rev. B **67**, 035318 (2003).
[4] T. Xu, M. P. Zach, Z. L. Xiao, D. Rosenmann, U. Welp, W. K. Kwok, and G. W. Crabtree, Appl. Phys. Lett. **86**, 203104 (2005).
[5] T. Kiefer, L. G. Villanueva, F. Fargier, F. Favier, and J. Brugger, Appl. Phys. Lett. **97**, 121911 (2010).
[6] N. Nakamura, T. Ueno, and H. Ogi, Appl. Phys. Lett. **114**, 201901 (2019).
[7] N. Nakamura, T. Ueno, and H. Ogi, J. Appl. Phys. **126**, 225104 (2019).
[8] E. Byon, T. W. H. Oates, and A. Anders, Appl. Phys. Lett. **82**, 1634 (2003).
[9] R. Abermann, R. Kramer, and J. Mäser, Thin Solid Films **52**, 215 (1978).
[10] F. Spaepen, Acta Mater. **48**, 31 (2000).
[11] E. Chason, B. W. Sheldon, L. B. Freund, J. A. Floro, and S. J. Hearne, Phys. Rev. Lett. **88**, 156103 (2002).
[12] G. Abadias, L. Simonot, J. J. Colin, A. Michel, S. Camelio, and D. Babonneau, Appl. Phys. Lett. **107**, 183105 (2015).
[13] J. Colin, A. Jamnig, C. Furgeaud, A. Michel, N. Pliatsikas, K. Sarakinos, and G. Abadias, Nanomaterials **10**, 2225 (2020).
[14] N. Nakamura and H. Ogi, Appl. Phys. Lett. **111**, 101902 (2017).
[15] N. Nakamura, N. Yoshimura, H. Ogi, and M. Hirao, J. Appl. Phys. **118**, 085302 (2015).
[16] F. Favier, E. C. Walter, M. P. Zach, T. Benter, and R. M. Penner, Science **293**, 2227 (2001).
[17] J. van Lith, A. Lassesson, S. A. Brown, M. Schulze, J. G. Partridge, and A. Ayesh, Appl. Phys. Lett. **91**, 181910 (2007).
[18] O. Dankert and A. Pundt, Appl. Phys. Lett. **81**, 1618 (2002).
[19] M. Zhao, M. H. Wong, and C. W. Ong, Appl. Phys. Lett. **107**, 033108 (2015).
[20] L. Zhou, N. Nakamura, A. Nagakubo, and H. Ogi, Appl. Phys. Lett. **115**, 171901 (2019).
[21] L. Zhou, F. Kato, N. Nakamura, Y. Oshikane, A. Nagakubo, and H. Ogi, Sens. Actuators, B **334**, 129651 (2021).
[22] H. Ogi, K. Motoshisa, T. Matsumoto, K. Hatanaka, and M. Hirao, Anal. Chem. **78**, 6903 (2006).